ground water

Evaluation of Noble Gas Recharge Temperatures in a Shallow Unconfined Aquifer

by Bradley D. Cey[1], G. Bryant Hudson[2], Jean E. Moran[3], and Bridget R. Scanlon[4]

Abstract

Water table temperatures inferred from dissolved noble gas concentrations (noble gas temperatures, NGT) are useful as a quantitative proxy for air temperature change since the last glacial maximum. Despite their importance in paleoclimate research, few studies have investigated the relationship between NGT and actual recharge temperatures in field settings. This study presents dissolved noble gas data from a shallow unconfined aquifer heavily impacted by agriculture. Considering samples unaffected by degassing, NGT calculated from common physically based interpretive gas dissolution models that correct measured noble gas concentrations for "excess air" agreed with measured water table temperatures (WTT). The ability to fit data to multiple interpretive models indicates that model goodness-of-fit does not necessarily mean that the model reflects actual gas dissolution processes. Although NGT are useful in that they reflect WTT, caution is recommended when using these interpretive models. There was no measurable difference in excess air characteristics (amount and degree of fractionation) between two recharge regimes studied (higher flux recharge primarily during spring and summer vs. continuous, low flux recharge). Approximately 20% of samples had dissolved gas concentrations below equilibrium concentration with respect to atmospheric pressure, indicating degassing. Geochemical and dissolved gas data indicate that saturated zone denitrification caused degassing by gas stripping. Modeling indicates that minor degassing ($<$10% ΔNe) may cause underestimation of ground water recharge temperature by up to 2°C. Such errors are problematic because degassing may not be apparent and degassed samples may be fit by a model with a high degree of certainty.

Introduction

Dissolved noble gases (He, Ne, Ar, Kr, and Xe) provide unique and valuable information in hydrologic studies. The conservative behavior of noble gases allows estimation of water table temperatures at the time of ground water recharge (noble gas temperatures, NGT) as well as ground water ages. NGT are particularly important in paleoclimate research for quantifying the temperature difference from the last glacial maximum (LGM, 23 to 18 ka BP) to present (e.g., Farrera et al. 1999). NGT are also used in studies to quantify mountain front/block recharge (e.g., Manning and Solomon 2005).

It is common for ground water to contain dissolved gas concentrations greater than equilibrium concentration with respect to atmospheric pressure. The additional dissolved gas is termed "excess air" because of its compositional similarity to air (Heaton and Vogel 1981). Some suggest that excess air may itself be a valuable paleoclimate proxy (Aeschbach-Hertig et al. 2002a; Castro et al. 2007).

NGT are much more sensitive to concentrations of heavier gases (e.g., Xe, Kr) because the solubility of these gases have much greater temperature dependency.

[1]Corresponding author: Department of Geological Sciences, Jackson School of Geosciences, University of Texas at Austin, 1 University Station C1100, Austin, TX 78712-0254; (512) 471-5172; fax (512) 471-9425; cey.home@gmail.com

[2]Chemical Sciences Division, Lawrence Livermore National Laboratory, Livermore, CA 94550

[3]Department of Earth and Environmental Sciences, California State University, East Bay, Hayward, CA 94542

[4]Bureau of Economic Geology, Jackson School of Geosciences, University of Texas at Austin, Austin, TX 78712

Received May 2008, accepted February 2009.

doi: 10.1111/j.1745-6584.2009.00562.x

In contrast, excess air is much more sensitive to concentrations of lighter gases (e.g., He, Ne) because lighter gases are only sparingly soluble (therefore additional dissolved gas causes a large relative change). Accurate determination of excess air is necessary for ground water age-dating using the ^3H–^3He technique (Solomon and Cook 2000). It is common to measure multiple gases to calculate NGT and excess air simultaneously using an error weighted inverse modeling procedure (Aeschbach-Hertig et al. 1999, 2000).

Despite the importance of NGT in paleoclimate research, few studies have attempted to experimentally confirm that NGT accurately reflect water table temperatures (WTT). This deficiency is critical given recent work examining assumptions in NGT calculations (Castro et al. 2007; Hall et al. 2005). Most noble gas studies report mean annual air temperature (MAAT) and the sampled water temperature. Because sampled wells are rarely screened across the water table, the sampled water temperature represents aquifer temperatures but not necessarily WTT. It is extremely rare for researchers to directly measure WTT in noble gas studies.

Holocher et al. (2002) completed a series of laboratory column experiments in which excess air was generated. The NGT matched the column temperature within measurement uncertainty for all samples. Stute and Sonntag (1992) investigated the relationship between NGT and subsurface temperature. NGT at a site near Bocholt, Germany, showed evidence of recharge from two areas (i.e., forest and field/meadow) having different soil thermal regimes. Subsurface temperature data from ~1 m above the water table were available from a nearby meteorological station having field/meadow vegetation. No temperature measurements for the forested area were reported. The NGT of ground water recharged in the field/meadow was the same as the measured soil temperature.

In a regional study, Castro et al. (2007) compared calculated NGT to recharge zone ground water temperatures. Although unable to match NGT to ground water temperature using common gas dissolution models, the NGT results matched ground water temperature if subsurface noble gas partial pressures were assumed to be greater than their respective atmospheric partial pressures. Subsurface noble gas partial pressures could be elevated relative to atmospheric conditions from O_2 consumption by biological processes and subsequent dissolution of the produced CO_2 (Stute and Schlosser 2000).

Klump et al. (2007) reported on field-scale noble gas dissolution experiments from two sites. In situ temperatures were not taken at the two study sites; however, subsurface temperatures were inferred from either measuring samples of recently recharged water or using data from a nearby (~20 km) meteorological station. They concluded that calculated NGT accurately reflected in situ soil temperatures.

In each of these three field studies, subsurface temperature data were considered in an attempt to compare NGT to WTT. However, none of these studies incorporated direct measurements of subsurface temperature to examine the relationship between NGT of very young (weeks to years) ground water to WTT.

The objectives of this study were to (1) compare modeled NGT to measured WTT to evaluate potential bias in NGT, (2) compare differences in gas dissolution occurring under two different recharge regimes (higher flux recharge primarily during spring and summer vs. continuous, low flux recharge), and (3) examine the potential impact of degassing on NGT. Improved understanding of gas dissolution processes occurring during ground water recharge will benefit ground water age-dating and paleoclimate studies. This study offers the following improvements over the noble gas studies discussed: (1) high frequency measurements of subsurface temperature throughout the unsaturated zone at multiple locations, (2) noble gas concentrations measured at multiple locations across the site, and (3) two different recharge regimes. This study complements recent work from the same site by Singleton et al. (2007) that focused on evidence for saturated zone denitrification and by McNab et al. (2007) that focused on the geochemistry of manure lagoon water. Singleton et al. (2007) present only averages of NGT and excess air for the site and calculate NGT using only Xe data. All analyses of dissolved noble gas data presented in this study are original—revised and expanded from the previous analyses by Singleton et al. (2007).

Materials and Methods

Study Site

The study site includes a dairy farm and surrounding fields in Kings County, California. The climate is Mediterranean type with hot summers and mild winters (MAAT = 16.6°C). Mean annual precipitation is 170 mm, with 80% falling during the coolest 5 months (November through March). Local meteorological data were obtained from a nearby (~10 km) National Climatic Data Center (NCDC) station. The site has minimal topographic relief (<2 m) and an elevation ~70 m above mean sea level. The local geology consists of unconsolidated sediments (primarily sands and silts) that were deposited in a series of alluvial fan systems originating where rivers exit the Sierra Nevada (Weissmann et al. 1999).

Cropland surrounding the dairy operation is flood irrigated with a combination of ground water and dairy wastewater (i.e., liquid manure). Occasionally water from the Kings River is transported through unlined canals for irrigation. Ground water used for irrigation is drawn from both a shallow perched aquifer (≤25 m below ground surface, bgs) and a deeper aquifer (≥40 m bgs). An unsaturated zone separates these two aquifers. Water for domestic use is drawn from the deep aquifer. The water table is ~5 m bgs across the site. Ground water flow direction within the perched aquifer is difficult to characterize because of many irrigation wells that pump intermittently and seasonally filled irrigation canals. Deeper regional ground water flow is generally westward toward

the center of the valley (Williamson et al. 1989). Additional details of the study site are given in McNab et al. (2007) and Singleton et al. (2007).

Five sets (locations 1S, 2S, 3S, 4S, and 6S) of small diameter multilevel wells were installed at the site (locations are given in Figure 1, depths are given in Table 1) as part of related studies (McNab et al. 2007; Singleton et al. 2007). These multilevel well sites are all located on the edges of flood irrigated fields alternatingly planted with corn and wheat, except 2S, which is beside an alfalfa field, and 6S, which is between cattle pens and manure lagoons. A sixth single completion well site (well 5S1) is located in a field ~11 m from the study area's main irrigation canal. This 14-m-wide canal is commonly full only during spring and summer months. All wells were 5 cm diameter, except 6S wells, which were 2.5 cm diameter. Screen lengths for these wells were 61 cm.

At three of the six well locations, additional unsaturated zone instrumentation was installed in February 2005. The three instrumented sites span the range of recharge conditions at the site: focused, higher flux recharge from irrigation canal leakage at 5S (recharge occurs during spring and summer only), and lower flux, relatively uniform recharge at 2S and 3S caused by regular flood irrigation. The 2S wells are away from irrigation wells, and 3S wells are between two irrigations wells (~25 and ~40 m away) that cause recurrent, local water table fluctuations. The instrumentation was placed at multiple depths in hand-augured boreholes to span the entire unsaturated zone at each location. Each borehole was instrumented with multiple sensors to record hourly measurements of soil temperature and matric potential (heat dissipation sensor model 229-L, Campbell Scientific Inc., Logan, Utah) and soil gas pressure (Druck barometer model RPT410F, Campbell Scientific Inc.). The approximate depths of heat dissipation sensors at each instrumented location were 0.4, 0.6, 0.9, 1.5, 2.4, and 3.9 m BGS. Before installation, heat dissipation sensors were calibrated using both pressure plate extractors and salt solutions (Scanlon et al. 2005).

Ground water samples were collected from multilevel wells using a portable, submersible pump (Grundfos™), with the exception of the smaller diameter 6S wells, which were sampled using a bladder pump. Ground water samples from multilevel wells were analyzed for pH in the field using a Horiba U-22 water quality meter. Cation and anion concentrations were measured by ion chromatography using a Dionex DX-600. Oxygen isotopic composition of water was measured using the carbon dioxide equilibration method for $^{18}O/^{16}O$ (Epstein and Mayeda 1953) on a VG Prism II isotope mass spectrometer.

Samples for dissolved noble gas analyses were collected in copper tubing sample vessels (8 mm inner diameter, 250 mm long). Steel clamps pinched the copper tubing flat in two locations to secure the water sample. Dissolved noble gas concentrations were measured as described in Cey et al. (2008). Analytical uncertainties are approximately 2% for He, Ne, and Ar and 3% for Kr and Xe.

All laboratory analyses of ground water samples were completed at Lawrence Livermore National Laboratory. The

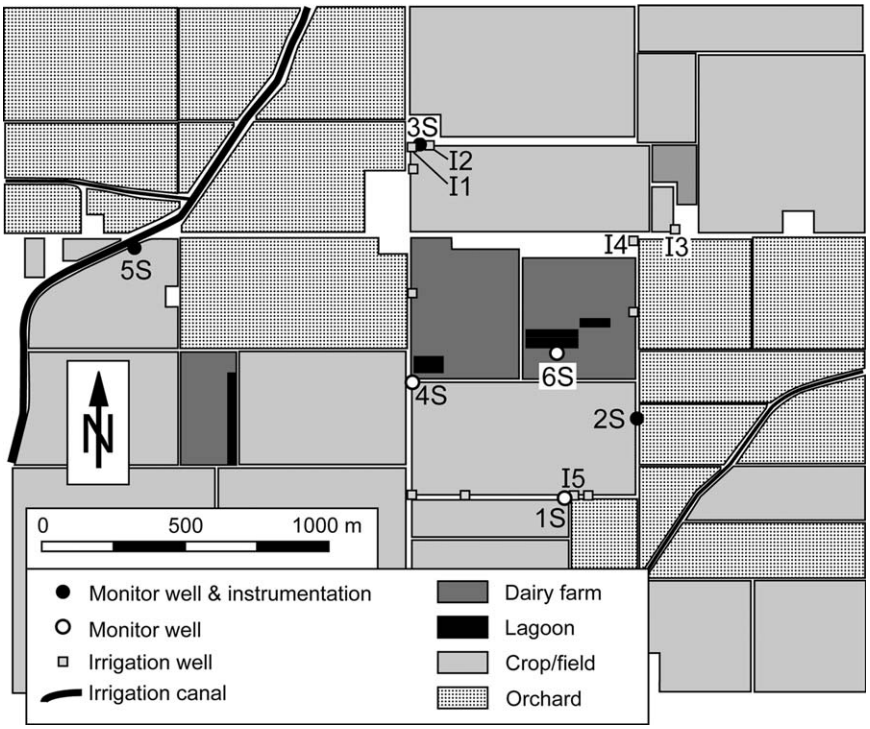

Figure 1. Map of study site. Only the sampled irrigation wells are uniquely labeled. Irrigation wells owned by other landowners are not shown.

Table 1
Well Depths, Sample Collection Dates, pH, Nitrate-N, Chloride, and $\delta^{18}O$

Well	Depth (m)[1]	Sample Number	Collection Date	pH (field)	NO_3^--N (mg/L)	Cl^- (mg/L)	$\delta^{18}O$ (‰)[2]
1S2	11.0	2250	12/6/04	7.05	0.07	46.3	–12.9
		2634	2/15/05	7.14	3.80	53.9	–12.8
		3065	7/11/05	–	3.64	57.3	–12.6
1S3	14.6	1864	1/10/04	6.65	0.03	23.4	–13.1
		1862	1/30/04	–	0.06	28.3	–13.0
		1871	2/13/04	6.77	0.06	31.3	–13.0
		1874	3/16/04	7.00	0.03	31.3	–12.9
		1880	4/20/04	7.10	0.05	41.0	–12.9
		1883	7/2/04	7.16	<0.02	46.1	–12.9
		2253	12/6/04	6.81	<0.02	41.7	–12.9
		2632	2/15/05	7.00	0.50	44.7	–12.9
1S4	19.8	1863	1/16/04	7.01	0.02	11.0	–13.3
		1866	1/30/04	–	0.34	9.6	–13.4
		1869	3/16/04	7.50	0.03	5.7	–13.3
		1873	4/20/04	7.50	0.05	5.9	–13.4
		1884	7/2/04	7.43	<0.02	8.2	–13.2
		2252	12/6/04	7.03	0.15	15.1	–13.3
		2631	2/15/05	7.30	0.10	13.4	–13.4
1S5	54.3	1865	1/16/04	9.50	0.04	2.0	–13.7
		1870	2/13/04	9.42	0.06	1.6	–13.8
		1868	3/16/04	9.30	0.03	1.9	–13.7
		2251	12/6/04	9.04	0.08	2.2	–13.7
2S1	5.5	3352	8/25/05	–	33.13	113.1	–12.4
2S2	9.5	2123	10/4/04	–	37.12	78.7	–12.1
		2259	12/7/04	6.50	45.50	120.8	–12.2
		2627	2/16/05	6.64	44.25	85.6	–12.2
2S3	11.1	2124	10/4/04	–	38.20	80.9	–12.2
		2628	2/15/05	–	45.12	90.1	–12.0
2S4	12.8	2125	10/4/04	–	1.06	72.4	–12.5
		2261	12/7/04	–	0.23	89.8	–12.4
		2633	2/15/05	6.97	3.51	55.9	–12.4
3S1	6.1	2258	12/7/04	6.60	37.02	116.4	–12.1
		2623	2/16/05	6.64	51.02	190.0	–11.7
		3070	7/11/05	–	49.60	204.7	–11.4
3S2	10.1	2257	12/7/04	6.58	57.36	257.1	–11.2
		3071	7/11/05	–	54.23	230.6	–11.1
3S3	12.3	2256	12/7/04	6.59	30.52	89.1	–12.3
3S4	14.4	2255	12/7/04	–	–	–	–11.7
4S1	6.4	2670	2/16/05	–	18.81	127.0	–
4S2	9.8	2264	12/8/04	6.93	27.56	32.4	–11.8
		2625	2/16/05	–	29.11	31.8	–11.8
4S3	10.8	2262	12/7/04	7.12	20.61	42.2	–12.0
		2636	2/17/05	7.27	14.21	42.4	–12.0
4S4	16.0	2263	12/8/04	6.98	<0.02	32.4	–13.0
5S1	4.9	2254	12/6/04	6.30	2.02	4.8	–14.2
		2626	2/17/05	6.32	9.91	17.2	–14.0
		2849	4/26/05	–	11.40	16.7	–14.0
		3068	7/11/05	–	8.67	19.4	–12.6
6S1	12.9	3348	8/25/05	–	0.06	152.6	–
6S2	11.0	3349	8/25/05	–	0.04	164.2	–
6S3	7.6	3350	8/25/05	–	32.05	154.0	–11.0
I1[3]	9.1	1889	5/28/04	6.83	36.53	113.4	–12.0
I2[3]	9.1	1890	5/28/04	6.73	15.42	127.7	–12.1
I3[3]		1771	8/21/03	–	<0.02	1.0	–13.7
I4[3]	9.1	1888	5/28/04	7.00	24.17	168.6	–9.9
I5[3]	10.7	1886	5/28/04	6.89	6.59	45.1	–12.4

[1]Depth to top of screen below ground surface, bgs.
[2]Parts per thousand relative to Vienna Standard Ocean Water, VSMOW.
[3]Irrigation well for which completion details are unavailable or unknown. Dashes indicate that measurements were not taken.

pH, chloride, and ^{18}O data presented here were previously reported by McNab et al. (2007), except for ^{18}O of lagoon water. The nitrate and dissolved noble gas data presented here were previously reported by Singleton et al. (2007).

Noble Gas Modeling

The equilibrium concentration, $C_{i,eq}$, of gas i is given by Henry's law as:

$$C_{i,eq} = \frac{p_i}{H_i(T,S)} \tag{1}$$

where p_i is partial pressure of gas i and H_i is Henry's law constant, which is a function of temperature T and salinity S. The total measured concentration, C_i, of dissolved gas i is the sum of multiple components:

$$C_i = C_{i,eq} + C_{i,exc} + C_{i,rad} + C_{i,ter} \tag{2}$$

where subscripts *exc*, *rad*, and *ter* refer to excess air, radiogenic, and terrigenic components, respectively.

Helium is commonly excluded from noble gas modeling because of complications that arise from the presence of radiogenic sources such as tritiogenic ^3He (Solomon and Cook 2000) or ^4He from U and Th decay (Solomon 2000). Calculation of equilibrium and excess air components of He is required to quantify tritiogenic ^3He, which is used to calculate ^3H–^3He ground water ages (Solomon and Cook 2000). Singleton et al. (2007) found only young (<50 years) ground water in the perched aquifer, which suggests negligible radiogenic components of ^4He, Ne, Ar, Kr, and Xe. It was assumed that ^4He, Ne, Ar, Kr, and Xe did not have significant radiogenic or terrigenic components in the study area (Lehmann et al. 1993); however, the deeper aquifer (well 1S5) may contain radiogenic ^4He.

Three physically based models are commonly used to interpret dissolved noble gas concentration data in ground water: (1) unfractionated air (UA) model (Heaton and Vogel 1981), (2) partial reequilibration (PR) model (Stute et al. 1995), and (3) closed system equilibrium (CE) model (Aeschbach-Hertig et al. 2000). The UA model is the simplest because it assumes the excess air component is atmospheric air resulting from complete dissolution of entrapped air bubbles during recharge. The total concentration of gas i as given by the UA model is:

$$C_i^{UA} = C_{i,eq} + A_d \cdot z_i \tag{3}$$

where A_d is concentration of dry air dissolved and z_i is volume fraction of gas i in dry air. Stute et al. (1995) postulated elemental fractionation in the excess air component (whereby lighter gases are depleted relative to heavier gases) and suggested that this fractionation was caused by complete bubble dissolution followed by diffusive degassing (PR model). The total concentration of gas i as given by the PR model is:

$$C_i^{PR} = C_{i,eq} + (A_d \cdot z_i) \cdot e^{\frac{-R^{PR} \cdot D_i}{D_{Ne}}} \tag{4}$$

where A_d is initial concentration of dissolved excess air, R^{PR} is degree of reequilibration, D_i is molecular diffusivity of gas i, and D_{Ne} is molecular diffusivity of Ne. Kipfer et al. (2002) extended the PR model to include multiple dissolution-degassing cycles. Aeschbach-Hertig et al. (2000) suggested that fractionation of excess air results from incomplete dissolution of entrapped air bubbles and fractionation is related to differing gas solubilities (CE model). The total concentration of gas i as given by the CE model is:

$$C_i^{CE} = C_{i,eq} + \frac{(1-F) \cdot A_e \cdot z_i}{1 + \left(\frac{F \cdot A_e \cdot z_i}{C_{i,eq}}\right)} \tag{5}$$

where F is a fractionation parameter and A_e is initial concentration of entrapped air:

$$A_e = \frac{V_g^0}{\rho(T,S) \cdot V_w} \cdot \frac{(P_g - e_s)}{P_0} \tag{6}$$

where $V_g{}^0$ is initial volume of entrapped air, ρ is water density as a function of temperature T and salinity S, V_w is volume of water, P_g is pressure of entrapped air, e_s is saturation water vapor pressure, and P_0 is standard pressure (1 atm). The fractionation parameter is:

$$F = \frac{v}{q} = \frac{\left(\frac{V_g}{V_g^0}\right)}{\left(\frac{P_g - e_s}{P_{atm} - e_s}\right)} \tag{7}$$

where V_g is volume of entrapped air, P_{atm} is atmospheric pressure, v is fraction of entrapped air remaining, and q is the ratio of dry entrapped air pressure to dry atmospheric pressure (which is approximately the pressure on the entrapped air).

The UA model is a limiting case for both the CE model (when $F = 0$) and the PR model (when $R^{PR} = 0$). CE and PR models can give similar results because underlying physical processes for these two models vary similarly among gases. Peeters et al. (2002) suggested that in addition to noble gas concentration data, isotopic data—especially Ne—are helpful in distinguishing between diffusive degassing (PR model) and incomplete bubble dissolution (CE model).

Addition of excess air has the greatest relative impact on He and Ne concentrations because the equilibrium component is relatively small. A common way to represent the amount of excess air is as percent Ne, ΔNe (Kipfer et al. 2002):

$$\Delta Ne = \frac{C_{Ne,exc}}{C_{Ne,eq}} \times 100\% \tag{8}$$

Dissolved gas concentrations may be reduced by degassing after recharge. Just as gas dissolution models are based on solubility (CE model) and diffusion (PR model), degassing can be controlled by solubility or diffusion. Such degassing occurs as a result of the formation of initially noble gas free gas bubbles (e.g., CO_2, CH_4, or N_2).

In the case of solubility controlled degassing occurring as a single step (DS1 model), the final degassed concentration of gas i is:

$$C_i^{DS1} = \frac{C_i^*}{1 + \frac{B \cdot z_i}{C_i^*}} \quad (9)$$

where C_i* is the initial (predegassing) concentration, B is a degassing parameter, and z_i is the concentration of gas i in air. This model is comparable to the CE model, except that the "entrapped air" of the CE model is free of noble gases in this case. This model was presented in Brennwald et al. (2003) as the "one-step degassing model." It can be extended to the case of repeated (continuous) gas bubble formation/equilibration (DSC model). The final degassed concentration is (equation 7 in Brennwald et al. [2005]):

$$C_i^{DSC} = C_i^* \cdot e^{\left(\frac{-Bz_i}{C_i^*}\right)} \quad (10)$$

Alternatively, degassing may be controlled by gas diffusion (DD model, Stute 1989). The final degassed concentration is:

$$C_i^{DD} = C_i^* \cdot e^{\left(-R^{DD}\frac{D_i}{D_{Ne}}\right)} \quad (11)$$

Diffusion controlled degassing is similar to the PR model; however, in this case, the dissolved gas diffuses into a reservoir that is initially free of noble gases. The limiting case of $R^{DD} \rightarrow \infty$ is therefore complete transfer of all noble gases from the water to the gas phase. In contrast, the limiting case of the PR dissolution model (when $R^{PR} \rightarrow \infty$) results in minimum gas concentrations equivalent to the equilibrium concentration with respect to atmospheric pressure.

Measured dissolved noble gas concentrations were modeled using NOBLE90, an error weighted, least-squares fitting, inverse modeling program (Aeschbach-Hertig et al. 1999; Peeters et al. 2002). NOBLE90 solves for parameter combinations for the selected interpretive model that match measured data within experimental error by minimizing χ^2, the sum of the weighted squared deviations between the modeled and measured concentrations. The ability of the selected model to describe the observed data (i.e., goodness-of-fit of the selected model) is judged on the probability of χ^2 being greater than a given value obtained from the χ^2 distribution (for the appropriate number of degrees of freedom). If this probability, p, is lower than a predetermined cutoff value, the solution is rejected and it is concluded that the selected model is unable to describe the measured data (Aeschbach-Hertig et al. 1999). This approach allows assessment of the likelihood that differences between modeled and measured values result from experimental error. In this study, solutions with $p < 0.05$ are rejected. The gas solubility data used in the NOBLE90 calculations were from multiple sources (Clever 1979; Weiss 1970, 1971; Weiss and Kyser 1978). Additional details of NOBLE90 are given by Aeschbach-Hertig et al. (1999, 2000) and Peeters et al. (2002). Measured He, Ne, Ar, Kr, and Xe concentrations were fitted by UA, PR, and CE models using NOBLE90 to solve for excess air, degree of excess air fractionation (in CE and PR models only), and recharge temperature. Additional modeling using only measured Ne, Ar, Kr, and Xe concentrations was also done. For all modeling, the recharging water was assumed to be fresh ($S = 0$) and the mean atmospheric pressure from the local NCDC meteorological station was used.

Degassing of ground water after recharge impacts interpreted (modeled) values of recharge temperature and excess air. Visser et al. (2007) examined the impact of saturated zone degassing on calculated ^{3}H–^{3}He ages, but did not model NGT. Aeschbach-Hertig et al. (2008) reported success in modeling undersaturated ground water samples from both the laboratory and a well using solubility-controlled degassing. To explore the impact of degassing on NGT, a separate modeling study was conducted. Hypothetical/synthetic dissolved noble gas data representative of site ground water conditions (T = 19.0°C, P_{atm} = 0.991 atm, $S = 0$, ΔNe = 30%) were generated—both unfractionated (UA model) and fractionated according to the CE model ($F = 0.65$ and 0.75). The representative gas concentrations were subsequently degassed by both the DS1 and DD models. The degree of degassing ranged from 0 to –10% ΔNe. The degassed samples were then modeled using the CE and UA models.

Results and Discussion

Soil-Gas Pressure

Soil-gas pressure data show pronounced diurnal and seasonal fluctuations (Figure 2). Atmospheric pressure data from the nearby NCDC station closely track the

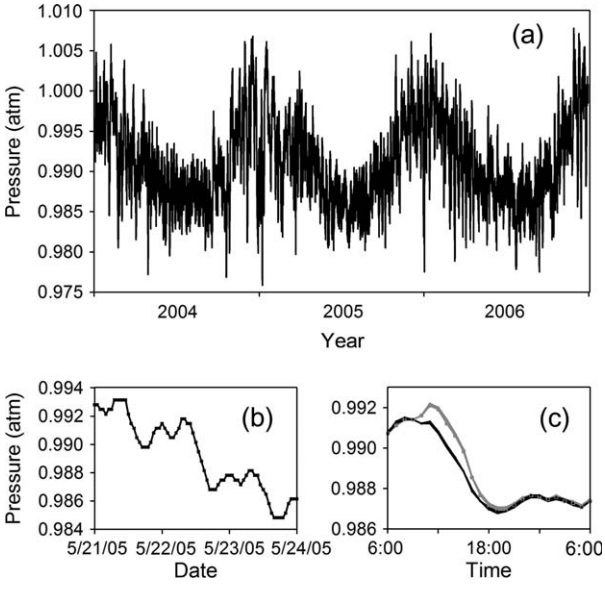

Figure 2. Atmospheric pressure data from nearby National Climatic Data Center (NCDC) station showing (a) seasonal fluctuations and (b) diurnal fluctuations. Panel (c) shows the impact of the May 22, 2005, irrigation event at 2S on soil-gas pressure (site 2S sensors: gray; sites 3S and 5S: black).

measured soil-gas pressures, with few exceptions. Each instance of soil-gas pressures deviating from atmospheric pressures can be linked to irrigation events during which soil-gas pressure beneath the irrigated field increased ~0.001 atm and subsequently dissipated in <12 h (Figure 2c). No measurable pressure gradient was found between the atmosphere and the unsaturated zone except during irrigation events, and no measurable vertical pressure gradient existed within the unsaturated zone during irrigation events.

Water Table

High frequency measurements of water table depth at all wells were not made. However, water table measurements made during sampling and matric potential measurements indicate that the water table beneath irrigated fields commonly rose by ~0.1 m in the days following an irrigation event. The annual water table range beneath irrigated fields was ~0.5 m. Because of its location between two irrigation wells, 3S responded differently. The water table at 3S was drawn down ~1 m during irrigation events.

When the irrigation canal adjacent to 5S1 was filled, there were small (<0.2 m) daily to weekly water table fluctuations at 5S1, most likely caused by the fluctuations in the canal's water level. The water table at 5S1 was lowest during winter (canal empty) and had an annual range ~1 m.

Temperature

Measured subsurface temperature data show both the lag and damping of seasonal temperature fluctuations with increasing depth in the soil column (Figure 3). Variations in WTT across the site (Figure 4) are likely related to differences in vegetation/crop type, irrigation (amount, timing, heating of irrigation water before infiltration), and depth to water table. Both 2S and 3S are located at the edges of irrigated fields. The 2S temperatures are higher than those at 3S and lag slightly (seasonal peaks occur later at 2S). The small lag difference is attributed to the water table at 2S being ~0.8 m deeper than at 3S. Higher temperatures at 2S are likely the result of greater heating of irrigation water before infiltration. Greater heating is caused by irrigation practices (water standing in 2S field longer) and location (2S is midway down the length of the field and 3S is at the end of the field from which water is applied). Virtually all irrigation events occurred when air temperatures were greater than WTT.

Oxygen Isotope Data ($\delta^{18}O$)

The $\delta^{18}O$ data cover a wide range, –14.2 to –9.9‰ (parts per thousand relative to Vienna Standard Mean Ocean Water, VSMOW) (Table 1). The 1S wells and 5S1 are unique in having relatively depleted ^{18}O values compared to other locations. Imported irrigation water is strongly depleted compared to local precipitation because imported irrigation water is from the Kings River, which is fed by Sierra Nevada snowmelt. The $\delta^{18}O$ range measured at 5S1 (adjacent to canal) is –14.2 to –12.6‰, which is essentially the same as that of Kings River water reported by Coplen and Kendall (2000) over a 4-year period (–14.6 to –12.5‰). The presence of depleted ^{18}O water at 5S1 confirms the importance of irrigation canal leakage as a recharge source.

The depleted ^{18}O at 1S wells may indicate a distinct recharge source because these wells have consistently low $\delta^{18}O$ despite not being located immediately adjacent to an

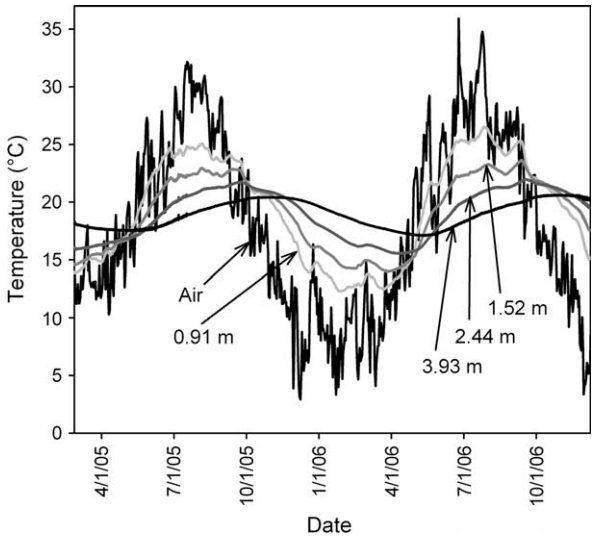

Figure 3. Subsurface temperature data from 3S location (sensors at 0.37 m and 0.61 m not shown). Local water table fluctuated between 3.8 and 5.5 m bgs during the study. Subsurface temperature data from the other instrumentation locations (2S and 5S) are similar. Air temperature data are from the nearby National Climatic Data Center (NCDC) station.

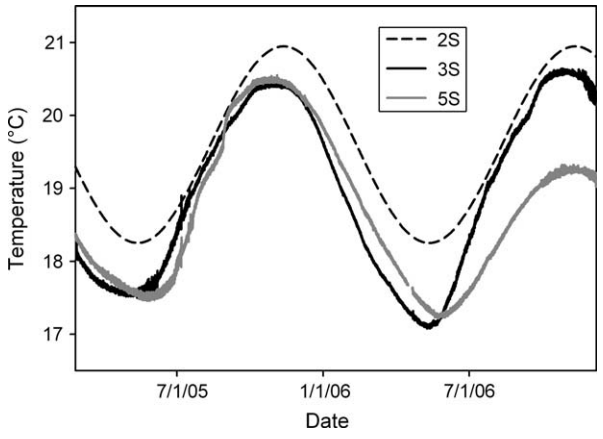

Figure 4. Water table temperatures for the three instrumented locations. Curves for 3S and 5S are data from the deepest heat dissipation sensor. The lower 2006 maximum temperature at 5S is attributed to increased vegetation cover in 2006. The curve for 2S is extrapolated from measured data using a sinusoidal curve and assuming exponential decay of the seasonal temperature signal with depth (water table was ~1.1 m below the deepest 2S sensor).

irrigation canal. The lack of variability of these samples may indicate a relative lack of mixing and therefore less impact by agricultural activity.

The most ^{18}O enriched monitoring well sample was 6S3 (–11.0‰), the shallowest monitoring well within the dairy farm operations area. The enrichment at 6S3 is likely caused by evaporative enrichment of nearby manure lagoon water (range –10.2 to –9.9‰, $n = 4$). Evaporative enrichment most likely occurs at manure lagoons as well as in the flood irrigated fields.

Repeated application of various different water types—shallow ground water, imported Kings River water, and liquid manure—to fields limits the use of ^{18}O in this study. However, the ^{18}O data verify the importance of irrigation canal leakage as a source of recharge. These data also suggest that imported water may be a significant contributor to 1S recharge.

Dissolved Noble Gases

Dissolved noble gas data were collected between August 2003 and August 2005 (Table 2). Analyses were completed on a number of duplicate samples. Some duplicate analyses did not reproduce initial results; however, results from individual wells were generally comparable (<10% difference), if not within the stated analytical uncertainty. The differences between duplicates are most likely associated with sampling rather than with laboratory analysis. Sampling ground water for dissolved gases is challenging at shallow depths because of low pore pressures. The differences in Kr and Xe between duplicates were most often minimal (less than analytical error); therefore the impact on calculated NGT was minimal.

Undersaturation

Several samples have gas concentrations below equilibrium gas solubility (e.g., samples from 1S2 and 2S4), indicative of degassing caused by gas stripping (i.e., removal of dissolved noble gases from solution by partitioning into an initially noble gas free bubble). The low measured gas concentrations are inconsistent with decreased equilibrium concentrations caused by high salinity, high temperature, or low pressure.

Many scenarios can result in ground water degassing by gas stripping. Denitrification-produced N_2 is reported in various studies to cause ground water degassing (Blicher-Mathiesen et al. 1998; Dunkle et al. 1993; Mookherji et al. 2003; Visser et al. 2007). Strongly anoxic conditions can lead to gas stripping by exsolution of methane (Fortuin and Willemsen 2005; Puckett et al. 2002). Methane production at hydrocarbon contaminated sites (Amos et al. 2005) and landfills (Solomon et al. 1992) can also cause degassing. Recent laboratory studies confirm the ability of biogenic gases to strip other gases from solution (Amos and Mayer 2006; Istok et al. 2007). Klump et al. (2006) reported slight undersaturation of dissolved gases in ground water and attributed it to gas stripping by CO_2 or CH_4 or both.

The location of subsurface gas production affects whether or not degassing occurs. If gas production occurs deep in the saturated zone, degassing is less likely to occur because increased hydrostatic pressure at greater depths forces the produced gas to remain in solution rather than form bubbles. However, if gas production occurs within a few meters of the water table, gas bubble formation is more likely (Visser et al. 2007). Because the main sources of gas production tend to be reactions in anoxic conditions (e.g., denitrification and methanogenesis), the shallower the redox cline, the more favorable it is for degassing to occur. The redox cline at this site is ~11 m bgs, which is ~6 m below the water table (Singleton et al. 2007).

There is no evidence for methanogenesis occurring in the shallow ground water; however, manure lagoon waters are methanogenic (McNab et al. 2007). McNab et al. (2007) suggested that observed Ar undersaturation in 2S samples is caused by CO_2 or CH_4 bubbles stripping previously dissolved gases within manure lagoon water before its infiltration. However, this explanation cannot account for the undersaturated samples at wells farther from the manure lagoons (e.g., samples from 3S4 and 5S1).

Ample evidence for denitrification at the site exists, but the observed N_2 excess caused by denitrification is less than expected for the observed nitrate concentration declines (Singleton et al. 2007). As Singleton et al. (2007) suggest, the lack of mass balance may be the result of N_2 loss from the saturated zone, which would strip noble gases from the ground water. Therefore, all samples below the zone of denitrification (generally 11 to 12 m bgs) may have undergone some degree of degassing. Such degassing may not be immediately noticeable if the initial excess air dissolved during recharge is greater than the amount of gas lost during degassing, but the interpreted recharge conditions could be inaccurate if degassing is not taken into account. Degassing by denitrification may help explain the measured undersaturation at 1S and 2S.

Gas stripping may be controlled by gas solubility (Equations 9 and 10) or by diffusion (Equation 11). The difference in gas concentrations between the processes is most relevant for light gases (i.e., He, Ne). The data suggest that solubility controlled degassing (DS1 and DSC models) occurs at 2S4 (Figure 5). There is also other evidence (stable isotopes of dissolved inorganic carbon) indicating that 2S is impacted by manure lagoon recharge (McNab et al. 2007), suggesting that some 2S4 degassing occurred within the manure lagoons before infiltration. There may be some diffusive degassing at other locations (e.g., 1S2); however, determination of the process causing degassing would benefit from isotopic analyses (Peeters et al. 2002).

The two undersaturated samples from 5S1 occurred during a time of little or no recharge (i.e., no irrigation in the nearby field and the canal had been empty for months). Samples from 5S1 taken when the canal was full were not undersaturated. There are no indications of reducing conditions at 5S1. Low nitrate concentrations are associated with low chloride (Table 1), indicating the dominance of low salinity recharge from the irrigation

Table 2
Dissolved Noble Gas Data

Well	Collection Date	Sample Number	Analysis Date	He[1] ($\times 10^{-8}$)	Ne[1] ($\times 10^{-7}$)	Ar[1] ($\times 10^{-4}$)	Kr[1] ($\times 10^{-8}$)	Xe[1] ($\times 10^{-8}$)
1S2	12/6/04	2250A	4/6/05	2.46	1.22	3.18	7.54	1.02
		2250B	4/19/05	2.41	1.19	3.18	7.46	1.08
	2/15/05	2634	4/6/05	2.32	1.18	3.05	7.35	0.994
	7/11/05	3065	9/30/05	2.52	1.32	3.18	7.40	1.00
1S3	1/16/04	1864A	2/27/04	7.57	2.96	4.13	8.86	1.17
		1864B	6/25/04	8.21	3.24	4.22	9.02	1.22
	1/30/04	1862A	2/27/04	5.89	2.48	3.99	8.44	1.15
		1862B	6/25/04	5.75	2.43	3.96	8.55	1.12
	2/13/04	1871A	3/27/04	5.26	2.25	3.81	8.27	1.17
		1871B	6/25/04	8.60	3.18	4.19	8.86	1.18
	3/16/04	1874A	3/24/04	5.44	2.27	3.92	8.52	1.16
		1874B	6/26/04	5.18	2.25	3.80	8.47	1.16
	4/20/04	1880A	4/23/04	5.04	2.21	3.89	8.62	1.15
		1880B	6/26/04	5.15	2.26	3.93	8.51	1.16
	7/2/04	1883	8/19/04	3.10	1.48	3.50	7.86	1.05
	12/6/04	2253	4/5/05	4.91	2.17	3.81	8.65	1.16
	2/15/05	2632	4/6/05	4.79	2.14	3.87	8.58	1.17
1S4	1/16/04	1863A	2/27/04	5.49	2.35	3.92	8.61	1.17
		1863B	6/25/04	7.33	3.00	4.08	8.72	1.16
	1/30/04	1866A	2/28/04	7.37	2.81	4.02	8.60	1.19
		1866B	6/25/04	7.35	2.82	4.02	8.75	1.19
	3/16/04	1869A	3/24/04	6.76	2.65	3.95	8.42	1.23
		1869B	6/26/04	6.64	2.67	3.86	8.39	1.12
	4/20/04	1873A	4/23/04	6.72	2.61	3.88	8.69	1.15
		1873B	6/26/04	6.68	2.62	3.88	8.41	1.17
	7/2/04	1884	8/19/04	6.52	2.46	3.79	8.33	1.09
	12/6/04	2252	4/6/05	6.42	2.49	3.75	8.34	1.13
	2/15/05	2631	3/25/05	6.25	2.47	3.83	8.41	1.11
1S5	1/16/04	1865	2/28/04	5.38	2.39	3.87	8.47	1.15
	2/13/04	1870A	2/27/04	12.16	3.43	3.85	8.45	1.17
		1870B	3/27/04	11.91	3.31	3.86	8.45	1.22
	3/16/04	1868	3/25/04	8.00	2.18	3.59	8.35	1.19
	12/6/04	2251	4/7/05	6.74	1.85	3.36	7.80	1.09
2S1	8/25/05	3352	9/8/05	4.79	2.24	3.34	7.48	0.990
2S2	10/4/04	2123	10/14/04	5.49	2.39	3.14	6.88	0.916
	12/7/04	2259A	2/10/05	5.25	2.26	3.13	6.88	0.923
		2259B	4/13/05	5.19	2.27	3.12	6.87	0.899
	2/16/05	2627	4/13/05	5.07	2.24	3.12	6.94	0.917
2S3	10/4/04	2124	10/14/04	3.65	1.78	2.99	6.77	0.879
	2/15/05	2628A	4/6/05	3.80	1.77	2.94	6.61	0.853
		2628B	4/13/05	2.69	1.36	2.68	6.29	0.869
2S4	10/4/04	2125	10/14/04	1.85	0.638	1.99	5.39	0.792
	12/7/04	2261	4/6/05	0.735	0.314	1.76	4.90	0.730
	2/15/05	2633A	4/6/05	0.864	0.375	1.82	5.11	0.735
		2633B	4/13/05	0.775	0.329	1.80	5.09	0.757
3S1	12/7/04	2258	2/9/05	4.62	2.08	3.38	7.54	0.984
	2/16/05	2623	3/25/05	4.93	2.12	3.45	7.60	0.983
	7/11/05	3070	9/30/05	5.14	2.37	3.46	7.67	1.01
3S2	12/7/04	2257	2/9/05	4.07	1.77	3.16	7.27	0.975
	7/11/05	3071	9/30/05	4.55	2.31	3.28	7.28	0.907
3S3	12/7/04	2256	2/9/05	4.99	2.16	3.54	7.91	1.03
3S4	12/7/04	2255	2/9/05	4.09	1.80	3.16	7.24	0.955
4S1	2/16/05	2670	4/7/05	4.61	1.99	3.25	7.23	0.947
4S2	12/8/04	2264	2/10/05	6.62	2.85	3.83	8.30	1.06
	2/16/05	2625	4/6/05	6.85	2.85	3.84	8.12	1.07
4S3	12/7/04	2262A	2/9/05	6.30	2.57	3.67	7.97	1.04
		2262B	4/19/05	6.77	2.72	3.72	8.12	1.03
	2/17/05	2636A	4/7/05	6.22	2.58	3.60	7.72	1.01
		2636B	4/7/05	6.41	2.70	3.65	7.77	1.01
4S4	12/8/04	2263A	2/9/05	4.42	2.36	3.66	7.59	1.00
		2263B	4/19/05	5.33	2.11	3.34	7.56	1.02
5S1	12/6/04	2254	4/5/05	3.82	1.68	3.19	7.48	1.02
	2/17/05	2626	4/6/05	4.03	1.74	3.09	7.23	0.990
	4/26/05	2849	5/17/05	4.38	1.89	3.32	7.49	1.00
	7/11/05	3068	9/30/05	5.69	2.44	3.62	7.93	1.05
I1	5/28/04	1889	6/29/04	9.30	3.75	4.36	8.76	1.08
I2	5/28/04	1890	6/29/04	7.73	2.92	3.79	8.14	0.993
I3	8/21/03	1771	11/26/03	6.42	2.10	3.64	8.66	1.21
I4	5/28/04	1888	6/29/04	13.4	5.07	5.03	9.57	1.14
I5	5/28/04	1886	6/29/04	10.4	4.02	4.40	8.76	1.15
ASW[2]	–	–	–	4.45	1.85	3.15	7.08	0.97

[1]Values given in cubic centimeters at standard temperature and pressure per gram water (cm^3 STP/g).
[2]Air saturated water (i.e., equilibrium concentration) at $T = 19.0°C$ and $P_{atm} = 0.991$ atm.

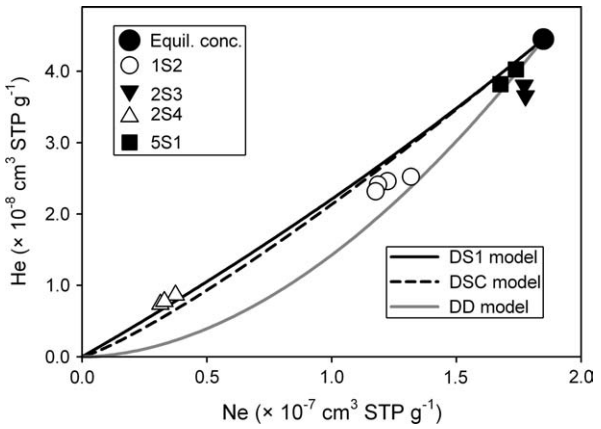

Figure 5. Helium vs. Ne concentrations of undersaturated samples. Equilibrium concentration given for T = 19°C, S = 0, P_{atm} = 0.991 atm. Lines show impact of degassing for each of the three degassing models.

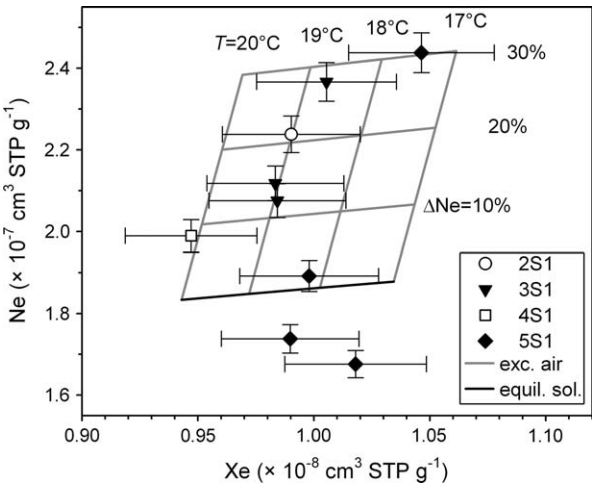

Figure 6. Ne and Xe concentrations of samples from the shallowest wells. Analytical uncertainties shown (Ne 2%, Xe 3%). Equilibrium solubilities from T = 17 to 20°C (S = 0, P_{atm} = 0.991 atm) are shown. Unfractionated excess air concentrations are also shown.

canal. Much of the land in the area is subject to intensive agriculture, including the application of cattle manure as fertilizer, which provides organic carbon. Undersaturation at 5S1 may be a result of gas stripping by CO_2; however, more detailed analyses are required to conclusively establish the cause of the undersaturation at this location.

Noble Gas Temperatures

The measured subsurface temperature data allow a direct comparison of modeled NGT to WTT. Ground water flows along complex and shifting paths because of intense but ephemeral pumping from relatively shallow irrigation wells in and around the study site. Therefore, it is particularly difficult to identify the recharge area for anything but the shallowest ground water. Furthermore, even if the recharge area of a deeper well were clearly identifiable, degassing could affect the calculation of NGT. For these reasons, samples from the shallowest well at each field location (wells 2S1, 3S1, 4S1, and 5S1) were considered separately.

The water table at the shallow wells was generally $\leq$ 2 m above the screens. There were no temperature sensors at 4S, but it is similar to locations 2S and 3S. Of the nine shallow well samples, two—both of which are from 5S1 when the canal was dry—are slightly undersaturated (Figure 6) and therefore are not discussed here. When modeled with all five gases (He, Ne, Ar, Kr, and Xe), none of the remaining seven samples was rejected as a poor fit by the PR model, but two of the seven samples were rejected as poor fits by the CE model (Figure 7 and Supporting Information Table S1). The superior fit of the PR model to the shallow well data suggests that some diffusive degassing may occur; however, isotope data are necessary to evaluate this (Peeters et al. 2002). Most studies report that the CE model gives a superior fit to the PR model (Kipfer et al. 2002). For those samples fit by both the CE and PR models, differences in NGT were small. The UA model produces systematically lower NGT than the CE or PR models (as discussed by Cey et al. [2008]). The DD model produces even lower NGT, which are generally lower than measured temperatures, indicating its inappropriateness for modeling these wells (Figure 7). It is clear that the ability of a given model to adequately fit measured data is not evidence that the model reflects the actual gas dissolution process (Aeschbach-Hertig et al. 2000; Cey et al. 2008).

The NGT of all shallow well samples are generally midrange of their WTT at each location, with the exception of 5S1 (Figure 7). Well 5S1 NGT are at the low end of the range of WTT, which is consistent with recharge occurring only during summer months when WTT are

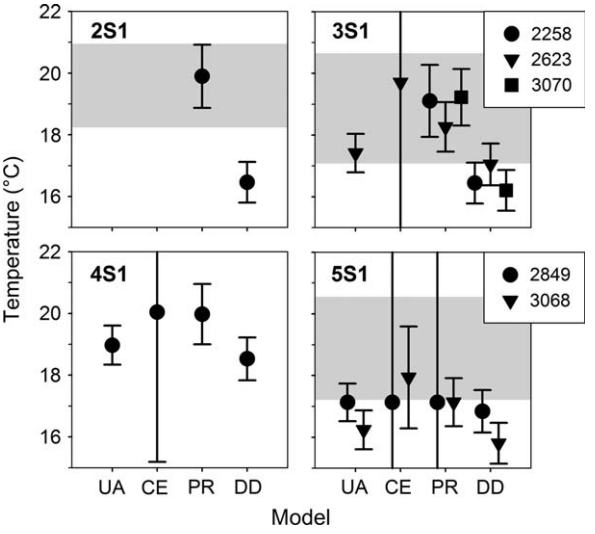

Figure 7. Noble gas temperatures (NGT) calculated for samples from the shallowest wells for four different models: unfractionated air (UA), closed system equilibrium (CE), partial re-equilibration (PR), and diffusive degassing (DD). The shaded region indicates the water table temperature (WTT) range for that location. For wells with multiple samples, the sample number is noted.

coolest (Figure 4). These results confirm the ability of NGT to match actual recharge temperatures.

Localized recharge conditions—such as strong seasonal variations in recharge as at the irrigation canal (i.e., 5S1)—are distinguishable based on NGT. The recharge regime at the canal is also unique because it consists of extended periods of either no recharge or consistent, relatively high head recharge. In contrast, the field sites have relatively uniform recharge flux as a result of many short-term recharge pulses (primarily irrigation events). The difference in recharge regimes was not apparent from the amount of excess air or the degree of fractionation.

There is uncertainty regarding the recharge location of the deeper wells. It is expected that ground water sampled in this study was recharged at or near the site under conditions similar to those measured at the site because land use in the vicinity of the site is representative of regional land use. The range of all WTT at the site is from ~17°C to ~21°C (Figure 4). The NGT are consistently midrange with the exception of 1S wells (Table S1). The average CE model NGT of 1S samples is 14.8°C compared with an average of 18.7°C for all other samples. Despite the difference in NGT, 1S samples are not distinctive in either their amount of excess air or their excess air fractionation. There is no evidence of unique agricultural practices near the 1S site, nor is there any evidence of pronounced differences in geology, but the possibility of localized spatial differences cannot be completely ruled out. Samples from 1S are more depleted in ^{18}O than virtually all other samples (Table 1). The low NGT and depleted ^{18}O—similar to well 5S1—suggest that the recharge source may be imported irrigation water. However, the NGT are still less than any WTT measured at the site. Irrigation lowers summertime ground temperature (Barnston and Schickedanz 1984; Bonfils and Lobell 2007), so it is possible that areas which recharge 1S wells could have different irrigation or cropping histories that depress WTT locally. Additionally, the modeled NGT may be erroneously low owing to partial degassing of the ground water after recharge (discussed in the following section). The exact cause of the low NGT is unclear, but it is clear based on dissolved noble gases and ^{18}O that 1S ground water is distinct from the ground water produced at the other well sites.

The ability of NGT from the CE and PR models to match measured WTT conditions at all but 1S confirms that the models are useful for the purposes of NGT calculation. The results of the PR and CE models are comparable, but additional data are required to establish the processes controlling gas dissolution. Caution is necessary when using such models to interpret dissolved gas data because goodness-of-fit is not an appropriate indicator of model validity.

Modeling Effects of Degassing on NGT

The impact of degassing on NGT was explored in a separate modeling exercise using hypothetical/synthetic dissolved noble gas data representative of measured data. The degree of degassing ranged from 0 to –10% ΔNe. The maximum degassing of –10% ΔNe is comparable to that associated with denitrification at the site based on the mass balance calculations of Singleton et al. (2007) (i.e., degassing caused by ~100 mg/L of nitrate denitrified ~6 m below the water table).

Results indicate that recharge temperature as fitted by the CE model can deviate appreciably from the original recharge temperature at modest levels of degassing (Figure 8a). The largest deviations are associated with (1) strong excess air fractionation and (2) diffusive degassing. The CE modeled recharge temperatures of the degassed samples underestimate the original recharge temperature for initially strongly fractionated excess air ($F = 0.75$), but not for less fractionated excess air ($F = 0.65$). The degree of fractionation is critical to the bias in modeled recharge temperature. Excess air fractionation during ground water recharge is common, with multiple studies reporting strongly fractionated excess air ($F > 0.7$)

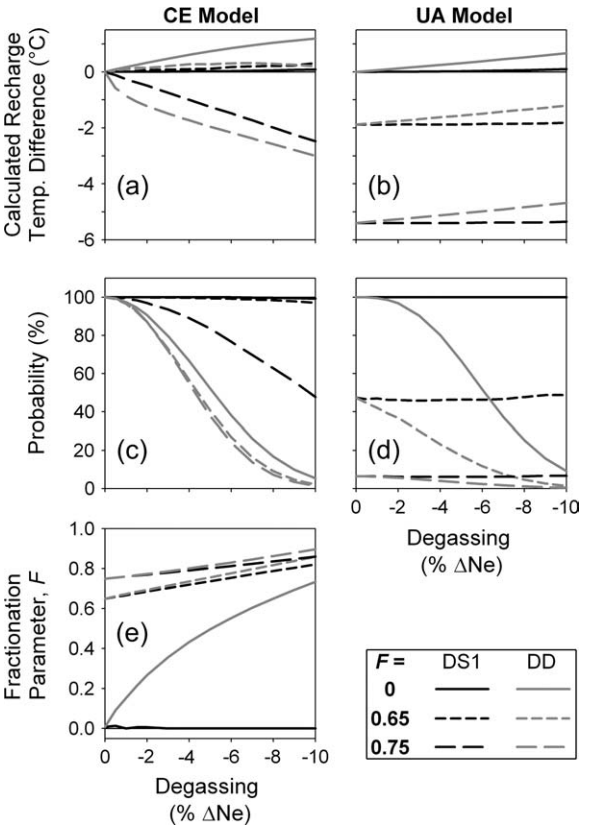

Figure 8. Impact of degassing on calculated NGT. These synthetic samples had excess air added (ΔNe = 30%), some unfractionated and others fractionated according to the CE model (both $F = 0.65$ and 0.75). Samples were then degassed by various amounts according to the DS1 and DD models. The resultant gas concentrations were then modeled by the CE and UA models. Panels (a) and (b) show the difference between original recharge temperature (19°C) and modeled recharge temperature after degassing. Panels (c) and (d) show model goodness-of-fit (probability of χ^2 being greater than a given value obtained from the χ^2 distribution for the appropriate number of degrees of freedom). Panel (e) shows the modeled CE fractionation parameter, F (note that the UA model is a limiting case of the CE model in which $F = 0$).

(Aeschbach-Hertig et al. 2000, 2002b; Hall et al. 2005). The errors in interpreted recharge temperature are slightly greater when degassing is controlled by diffusion rather than solubility. The prevalence of diffusive degassing is uncertain, because most studies indicate that gas solubility rather than diffusion controls both dissolution (Kipfer et al. 2002) and degassing (Visser et al. 2007). However, there is some evidence for diffusive degassing at this site based on elemental ratios (1S2, Figure 5).

As shown in this study and in previous work (Blicher-Mathiesen et al. 1998; Dunkle et al. 1993; Fortuin and Willemsen 2005; Klump et al. 2006; Mookherji et al. 2003; Puckett et al. 2002; Visser et al. 2007), ground water degassing can occur in a variety of settings. Minor degassing in the saturated zone after ground water recharge may help explain the NGT biases reported by Castro et al. (2007) and Hall et al. (2005).

Application of an incorrect interpretive model can result in substantial error in the modeled recharge temperature, especially for samples with strongly fractionated excess air (Figure 8b). The UA model systematically calculates lower recharge temperatures than the CE model (Aeschbach-Hertig et al. 2000; Cey et al. 2008); therefore, modeling samples with fractionated excess air using the UA model results in underestimation of recharge temperature. This is true regardless of the amount of degassing, including the case of no degassing.

Caution is necessary when applying interpretive models to deduce recharge temperature from dissolved noble gas data. Application of a model that is not representative of the actual gas dissolution process may yield erroneous results. The occurrence of degassing after recharge may also result in erroneous recharge temperatures. Model goodness-of-fit is not necessarily indicative of model appropriateness (Figure 8c and Figure 8d). Even models that match measured data well may be seriously biased.

Conclusions

The study examined dissolved noble gases in shallow ground water at an agricultural site. The local hydrologic regime is heavily impacted by both pumping of ground water from a shallow unconfined aquifer and importation of surface water for irrigation. Measurements of soil-gas pressure and subsurface temperature defined conditions under which recharge occurred.

Samples from multiple wells had dissolved gas concentrations below equilibrium concentration with respect to atmospheric pressure. The most plausible explanation for the undersaturated samples is degassing caused by gas stripping. Multiple gas stripping processes occur at the site (1) within methanogenic liquid manure lagoons, which subsequently recharge, and (2) in the saturated zone because of denitrification and possibly also CO_2 exsolution. The degassing observed has the potential to bias NGT. Hypothetical samples were modeled to explore the possible effect of degassing on interpreted NGT. Results indicate that relatively minor degassing ($<10\%$ ΔNe) may cause bias of 2°C. Such errors are problematic because the degassing may be masked by excess air and the degassed samples may be fit by a model with a high degree of certainty. These findings have implications for paleoclimate research because based on NGT data the temperature difference since the LGM is 5°C to 7°C (Kipfer et al. 2002). Therefore, caution is necessary when using NGT in paleoclimate work.

The role of recharge regime on dissolved noble gases was also examined. There are two recharge regimes occurring at the study site: (1) focused, higher flux recharge from irrigation canal leakage during spring and summer only (little to no recharge in fall and winter) and (2) lower flux, spatially and temporally uniform recharge caused by regular flood irrigation. There was no measurable difference in excess air characteristics (amount and degree of fractionation) between the two recharge regimes studied.

The study examined the relationship between calculated NGT based on dissolved noble gases and directly measured WTT. The complexity of ground water flow and the potential for degassing to affect NGT required that only shallow wells be used to compare NGT to WTT. The NGT from both the CE and PR models reflect the measured WTT conditions. This finding supports the use of dissolved noble gases to deduce recharge temperatures. Before this study, field-based experimental confirmation was lacking despite decades of NGT applications.

Although NGT reflect WTT, careful application of interpretive models is required because multiple gas dissolution/exsolution processes may contribute to measured dissolved gas concentrations in ground water. A particular model may be fit to measured data, but this does not necessarily mean that the physical gas dissolution process is accurately represented or that the model results accurately represent recharge conditions. Therefore, caution is necessary when interpreting dissolved noble gas data.

Acknowledgments

Funding was provided by the California State Water Resources Control Board Groundwater Ambient Monitoring and Assessment (GAMA) Program, Lawrence Livermore National Laboratory, the Jackson School of Geosciences, and the Glenn T. Seaborg Institute (fellowship to B.D.C.). We acknowledge Dr. Brad Esser for his sustained support of the project, Dr. Mike Singleton for assistance with sampling and analyses, Mr. Wayne Culham for assistance with sample analyses, and the landowner for access to the study site. This paper benefited from the insightful and constructive comments of Drs. Kip Solomon and Stephen van der Hoven, and two anonymous reviewers.

Supporting Information

Additional Supporting Information may be found in the online version of this article:

Table S1. Results of Noble Gas Monitoring.

[Corrections added after online publication March 26, 2009: on page 1, the table was incorrectly labeled as a

"Results of Noble Bas Monitoring", but should have been labeled as a "Results of Noble Gas Monitoring"; on page 1, "Modeling &q1;was done" was incorrect and should have been "Modeling was done". We apologize for these errors.]

Please note: Wiley-Blackwell are not responsible for the content or functionality of any supporting materials supplied by the authors. Any queries (other than missing material) should be directed to the corresponding author for the article.

References

Aeschbach-Hertig, W., H. El-Gamal, M. Wieser, and L. Palcsu. 2008. Modeling excess air and degassing in groundwater by equilibrium partitioning with a gas phase. *Water Resources Research* 44, no. 8: W08449, doi:08410.01029/02007WR006454.

Aeschbach-Hertig, W., U. Beyerle, and R. Kipfer. 2002a. Excess air in groundwater as a proxy for paleo-humidity. In *12th Annual V. M. Goldschmidt Conference*, *Davos, Switzerland.* Geochimica et Cosmochimica Acta 66, Supp. 1 [abstracts].

Aeschbach-Hertig, W., M. Stute, J.F. Clark, R.F. Reuter, and P. Schlosser. 2002b. A paleotemperature record derived from dissolved noble gases in groundwater of the Aquia Aquifer (Maryland, USA). *Geochimica et Cosmochimica Acta* 66, no. 5: 797–817.

Aeschbach-Hertig, W., F. Peeters, U. Beyerle, and R. Kipfer. 2000. Palaeotemperature reconstruction from noble gases in ground water taking into account equilibration with entrapped air. *Nature* 405, no. 6790: 1040–1044.

Aeschbach-Hertig, W., F. Peeters, U. Beyerle, and R. Kipfer. 1999. Interpretation of dissolved atmospheric noble gases in natural waters. *Water Resources Research* 35, no. 9: 2779–2792.

Amos, R.T., and K.U. Mayer. 2006. Investigating ebullition in a sand column using dissolved gas analysis and reactive transport modeling. *Environmental Science and Technology* 40, no. 17: 5361–5367.

Amos, R.T., K.U. Mayer, B.A. Bekins, G.N. Delin, and R.L. Williams. 2005. Use of dissolved and vapor-phase gases to investigate methanogenic degradation of petroleum hydrocarbon contamination in the subsurface. *Water Resources Research* 41, no. 2: W02001, doi:02010.01029/02004WR003433.

Barnston, A.G., and P.T. Schickedanz. 1984. The effect of irrigation on warm season precipitation in the southern Great Plains. *Journal of Climate and Applied Meteorology* 23, no. 6: 865–888.

Blicher-Mathiesen, G., G.W. McCarty, and L.P. Nielsen. 1998. Denitrification and degassing in groundwater estimated from dissolved dinitrogen and argon. *Journal of Hydrology* 208, no. 1–2: 16–24.

Bonfils, C., and D. Lobell. 2007. Empirical evidence for a recent slowdown in irrigation-induced cooling. *Proceedings of the National Academy of Sciences* 104, no. 34: 13582–13587.

Brennwald, M.S., R. Kipfer, and D.M. Imboden. 2005. Release of gas bubbles from lake sediment traced by noble gas isotopes in the sediment pore water. *Earth and Planetary Science Letters* 235, no. 1–2: 31–44.

Brennwald, M.S., M. Hofer, F. Peeters, W. Aeschbach-Hertig, K. Strassmann, R. Kipfer, and D.M. Imboden. 2003. Analysis of dissolved noble gases in the pore water of lacustrine sediments. *Limnology and Oceanography: Methods* 1, 51–62.

Castro, M.C., C.M. Hall, D. Patriarche, P. Goblet, and B.R. Ellis. 2007. A new noble gas paleoclimate record in Texas—Basic assumptions revisited. *Earth and Planetary Science Letters* 257, no. 1–2: 170–187.

Cey, B.D., G.B. Hudson, J.E. Moran, and B.R. Scanlon. 2008. Impact of artificial recharge on dissolved noble gases in groundwater in California. *Environmental Science and Technology* 42, no. 4: 1017–1023.

Clever, H.L., ed. 1979. *Krypton, Xenon and Radon*. Elmsford, New York: Pergamon Press.

Coplen, T.B., and C. Kendall. 2000. Stable hydrogen and oxygen isotope ratios for selected sites of the U.S. Geological Survey's NASQAN and benchmark surface-water networks. U.S. Geological Survey Open-File Report 00-160. Reston, Virginia: USGS.

Dunkle, S.A., L.N. Plummer, E. Busenberg, P.J. Phillips, J.M. Denver, P.A. Hamilton, R.L. Michel, and T.B. Coplen. 1993. Chlorofluorocarbons (CCl_3F and CCl_2F_2) as dating tools and hydrologic tracers in shallow groundwater of the Delmarva Peninsula, Atlantic Coastal Plain, United States. *Water Resources Research* 29, no. 12: 3837–3860.

Epstein, S., and T.K. Mayeda. 1953. Variation of ^{18}O content of waters from natural sources. *Geochimica et Cosmochimica Acta* 4, no. 5: 213–224.

Farrera, I., S.P. Harrison, I.C. Prentice, G. Ramstein, J. Guiot, P.J. Bartlein, R. Bonnefille, M. Bush, W. Cramer, U. von Grafenstein, K. Holmgren, H. Hooghiemstra, G. Hope, D. Jolly, S.-E. Lauritzen, Y. Ono, S. Pinot, M. Stute, and G. Yu. 1999. Tropical climates at the last glacial maximum: A new synthesis of terrestrial paleoclimate data. I. Vegetation, lake-levels and geochemistry. *Climate Dynamics* 15, no. 11: 823–856.

Fortuin, N.P.M., and A. Willemsen. 2005. Exsolution of nitrogen and argon by methanogenesis in Dutch ground water. *Journal of Hydrology* 301, no. 1–4: 1–13.

Hall, C.M., M.C. Castro, K.C. Lohmann, and L. Ma. 2005. Noble gases and stable isotopes in a shallow aquifer in southern Michigan: Implications for noble gas paleotemperature reconstructions for cool climates. *Geophysical Research Letters* 32, no. 18: L18404, doi:18410.11029/12005GL023582.

Heaton, T.H.E., and J.C. Vogel. 1981. "Excess air" in groundwater. *Journal of Hydrology* 50, no. 1–3: 201–216.

Holocher, J.O., F. Peeters, W. Aeschbach-Hertig, M. Hofer, M. Brennwald, W. Kinzelbach, and R. Kipfer. 2002. Experimental investigations on the formation of excess air in quasi-saturated porous media. *Geochimica et Cosmochimica Acta* 66, no. 23: 4103–4117.

Istok, J.D., M.M. Park, A.D. Peacock, M. Oostrom, and T.M. Wietsma. 2007. An experimental investigation of nitrogen gas produced during denitrification. *Ground Water* 45, no. 4: 461–467.

Kipfer, R., W. Aeschbach-Hertig, F. Peeters, and M. Stute. 2002. Noble gases in lakes and ground waters. In *Noble Gases in Geochemistry and Cosmochemistry*, ed. D. Porcelli, C. J. Ballentine, and R. Wieler, 615–700. Washington, DC: Mineralogical Society of America.

Klump, S., Y. Tomonaga, P. Kienzler, W. Kinzelbach, T. Baumann, D.M. Imboden, and R. Kipfer. 2007. Field experiments yield new insights into gas exchange and excess air formation in natural porous media. *Geochimica et Cosmochimica Acta* 71, no. 6: 1385–1397.

Klump, S., R. Kipfer, O.A. Cirpka, C.F. Harvey, M.S. Brennwald, K.N. Ashfaque, A.B.M. Badruzzaman, S.J. Hug, and D.M. Imboden. 2006. Groundwater dynamics and arsenic mobilization in Bangladesh assessed using noble gases and tritium. *Environmental Science and Technology* 40, no. 1: 243–250.

Lehmann, B.E., S.N. Davis, and J.T. Fabryka-Martin. 1993. Atmospheric and subsurface sources of stable and radioactive nuclides used for groundwater dating. *Water Resources Research* 29, no. 7: 2027–2040.

Manning, A.H., and D.K. Solomon. 2005. An integrated environmental tracer approach to characterizing groundwater circulation in a mountain block. *Water Resources Research* 41, no. 12: W12412, doi:12410.11029/12005WR004178.

McNab, W.W., M.J. Singleton, J.E. Moran, and B.K. Esser. 2007. Assessing the impact of animal waste lagoon seepage on the geochemistry of an underlying shallow aquifer. *Environmental Science and Technology* 41, no. 3: 753–758.

Mookherji, S., G.W. McCarty, and J.T. Angier. 2003. Dissolved gas analysis for assessing the fate of nitrate in wetlands. *Journal of the American Water Resources Association* 39, no. 2: 381–387.

Peeters, F., U. Beyerle, W. Aeschbach-Hertig, J.O. Holocher, M.S. Brennwald, and R. Kipfer. 2002. Improving noble gas based paleoclimate reconstruction and groundwater dating using $^{20}Ne/^{22}Ne$ ratios. *Geochimica et Cosmochimica Acta* 67, no. 4: 587–600.

Puckett, L.J., T.K. Cowdery, P.B. McMahon, L.H. Tornes, and J.D. Stoner. 2002. Using chemical, hydrologic, and age dating analysis to delineate redox processes and flow paths in the riparian zone of a glacial outwash aquifer-stream system. *Water Resources Research* 38, no. 8: 1134, doi:1110.1029/2001WR000396.

Scanlon, B.R., R.C. Reedy, K.E. Keese, and S.F. Dwyer. 2005. Evaluation of evapotranspirative covers for waste containment in arid and semiarid regions in the southwestern USA. *Vadose Zone Journal* 4, no. 1: 55–71.

Singleton, M.J., B.K. Esser, J.E. Moran, G.B. Hudson, W.W. McNab, and T. Harter. 2007. Saturated zone denitrification: Potential for natural attenuation of nitrate contamination in shallow groundwater under dairy operations. *Environmental Science and Technology* 41, no. 3: 759–765.

Solomon, D.K. 2000. ^{4}He in groundwater. In *Environmental Tracers in Subsurface Hydrology*, ed. P.G. Cook and A.L. Herczeg, 425–439. Norwell, Massachusetts: Kluwer Academic Publishers.

Solomon, D.K., and P.G. Cook. 2000. ^{3}H and ^{3}He. In *Environmental Tracers in Subsurface Hydrology*, ed. P.G. Cook and A.L. Herczeg, 397–424. Norwell, Massachusetts: Kluwer Academic Publishers.

Solomon, D.K., R.J. Poreda, S.L. Schiff, and J.A. Cherry. 1992. Tritium and helium 3 as groundwater age tracers in the Borden Aquifer. *Water Resources Research* 28, no. 3: 741–755.

Stute, M.1989. Edelgase im Grundwasser – Bestimmung von Paläotemperaturen und Untersuchung der Dynamik von Grundwasserfliessystemen [Noble gases in groundwater – regulation of paleotemperature and investigation of the dynamics of groundwater flow systems]. Ph.D. diss, Universität Heidelberg.

Stute, M., and P. Schlosser. 2000. Atmospheric noble gases. In *Environmental Tracers in Subsurface Hydrology*, ed. P.G. Cook and A.L. Herczeg, 349–377. Norwell, Massachusetts: Kluwer Academic Publishers.

Stute, M., M. Forster, H. Frischkorn, A. Serejo, J.F. Clark, P. Schlosser, W.S. Broecker, and G. Bonani. 1995. Cooling of tropical Brazil (5°C) during the last glacial maximum. *Science* 269, no. 5222: 379–383.

Stute, M., and C. Sonntag. 1992. Palaeotemperatures derived from noble gases dissolved in groundwater and in relation to soil temperature. In *Isotopes of Noble Gases as Tracers in Environmental Studies*, Vienna, 29 May-2 June 1989, 111–122. http://www.iaea.org/programmes/ripc/ih/publications/stable_isotope.htm.

Visser, A., H.P. Broers, and M.F.P. Bierkens. 2007. Dating degassed groundwater with $^{3}H/^{3}He$. *Water Resources Research* 43, no. 10: W10434, doi:10410.11029/12006WR005847.

Weiss, R.F. 1971. Solubility of helium and neon in water and seawater. *Journal of Chemical and Engineering Data* 16, no. 2: 235–241.

Weiss, R.F. 1970. The solubility of nitrogen, oxygen and argon in water and seawater. *Deep-Sea Research* 17, no. 4: 721–735.

Weiss, R.F., and T.K. Kyser. 1978. Solubility of krypton in water and seawater. *Journal of Chemical and Engineering Data* 23, no. 1: 69–72.

Weissmann, G.S., S.F. Carle, and G.E. Fogg. 1999. Three-dimensional hydrofacies modeling based on soil surveys and transition probability geostatistics. *Water Resources Research* 35, no. 6: 1761–1770.

Williamson, A.K., D.E. Prudic, and L.A. Swain. 1989. Groundwater flow in the Central Valley, California. U.S. Geological Survey Professional Paper 1401-D. Reston, Virginia: USGS.

Supporting Information for:

Cey et al. 2009, Evaluation of Noble Gas Recharge Temperatures in a Shallow Unconfined Aquifer

Table S1. Results of noble gas modeling. Modeling was done using He, Ne, Ar, Kr, and Xe for the UA, PR, and CE models. Additional modeling was done using only Ne, Ar, Kr, and Xe with the CE model. Results rejected because of poor fitting (i.e. $p < 0.05$) are not shown. Samples with large recharge temperature uncertainties are included despite the obvious non-uniqueness of the result.

		UA				PR					CE					CE (excluding He)				
Well	**Sample**	***p***	***T* (°C)**	**+/- (°C)**	**ΔNe (%)**	***p***	***T* (°C)**	**+/- (°C)**	**ΔNe (%)**	***R***	***p***	***T* (°C)**	**+/- (°C)**	**ΔNe (%)**	***F***	***p***	***T* (°C)**	**+/- (°C)**	**ΔNe (%)**	***F***
1S2	2250A	0.00	-	-	-	0.00	-	-	-	-	0.00	-	-	-	-	0.00	-	-	-	-
	2250B	0.00	-	-	-	0.00	-	-	-	-	0.00	-	-	-	-	0.00	-	-	-	-
	2634	0.00	-	-	-	0.00	-	-	-	-	0.00	-	-	-	-	0.00	-	-	-	-
	3065	0.00	-	-	-	0.00	-	-	-	-	0.00	-	-	-	-	0.00	-	-	-	-
1S3	1864A	0.06	13.1	0.6	26	0.10	13.7	0.7	30	0.24	0.77	16.3	2.5	31	0.71	0.56	16.3	2.4	31	0.70
	1864B	0.02	-	-	-	0.03	-	-	-	-	0.76	17.8	5.6	29	0.75	0.90	19.5	22.8	32	0.74
	1862A	0.65	13.7	0.6	54	0.44	13.7	0.7	54	0.00	0.62	14.6	1.2	56	0.27	0.71	15.0	1.4	55	0.38
	1862B	0.99	13.4	0.7	66	1.00	13.5	0.8	67	0.03	0.98	13.6	1.1	67	0.09	0.95	13.5	1.2	67	0.04
	1871A	0.31	13.0	0.6	14	0.40	13.4	0.7	17	0.31	0.62	14.6	2.0	16	0.82	0.43	14.6	1.8	17	0.80
	1871B	0.33	14.4	0.7	70	0.09	14.2	0.8	67	0.00	0.15	14.3	1.1	69	0.00	0.93	14.9	1.3	66	0.24
	1874A	0.14	12.6	0.6	16	0.08	12.8	0.7	18	0.15	0.85	16.5	7.5	21	0.81	0.57	16.4	11.9	21	0.81
	1874B	0.23	12.8	0.6	13	0.58	13.4	0.7	17	0.44	0.58	14.7	2.4	16	0.83	0.94	14.7	2.0	17	0.80
	1880A	0.02	-	-	-	0.08	13.0	0.7	15	0.65	0.18	14.7	6.2	14	0.87	0.38	16.1	20.0	18	0.84
	1880B	0.01	-	-	-	0.07	13.1	0.7	18	0.59	0.17	14.9	5.1	16	0.84	0.40	16.3	13.3	20	0.82
	1883	0.00	-	-	-	0.00	-	-	-	-	0.00	-	-	-	-	0.00	-	-	-	-
	2253	0.08	12.3	0.6	8	0.31	13.0	0.7	13	0.78	0.23	14.1	5.4	11	0.89	0.58	15.7	14.9	15	0.87
	2632	0.02	-	-	-	0.17	12.9	0.8	11	1.20	0.07	13.4	5.6	8	0.92	0.31	14.8	17.5	13	0.88
1S4	1863A	0.13	12.4	0.6	18	0.23	13.0	0.7	22	0.31	0.80	15.2	2.9	22	0.78	0.93	15.3	2.6	23	0.77
	1863B	0.42	14.0	0.6	53	0.80	14.6	0.8	57	0.13	0.80	15.4	1.3	56	0.36	0.83	15.2	1.3	57	0.29
	1866A	0.54	13.9	0.6	49	0.21	13.7	0.7	47	0.00	0.29	13.8	1.0	48	0.00	0.68	14.2	1.3	46	0.30
	1866B	0.69	13.7	0.6	49	0.34	13.6	0.7	47	0.00	0.42	13.7	1.0	48	0.00	0.93	14.0	1.2	46	0.28
	1869A	0.49	13.3	0.6	38	0.24	13.2	0.7	37	0.00	0.23	13.3	1.0	37	0.00	0.19	13.2	1.2	36	0.00
	1869B	0.83	14.9	0.6	39	0.73	15.1	0.7	40	0.05	0.94	15.7	1.3	41	0.39	0.77	15.8	1.4	41	0.42
	1873A	0.55	14.1	0.6	38	0.27	14.0	0.7	37	0.00	0.33	14.1	1.0	37	0.00	0.42	14.6	1.3	36	0.45
	1873B	0.86	14.2	0.6	38	0.60	14.1	0.7	37	0.00	0.66	14.1	1.0	37	0.00	0.70	14.4	1.2	36	0.32
	1884	0.08	15.4	0.6	34	0.02	-	-	-	-	0.03	-	-	-	-	0.55	17.0	1.8	31	0.67
	2252	0.64	14.9	0.6	33	0.28	14.6	0.7	31	0.00	0.34	14.9	1.0	32	0.00	0.75	15.0	1.2	30	0.37
	2631	0.43	14.6	0.6	31	0.24	14.6	0.7	30	0.00	0.35	15.7	1.3	33	0.54	0.62	16.4	1.7	31	0.66
1S5	1865	0.01	-	-	-	0.48	14.0	0.7	25	0.56	0.13	15.3	2.4	22	0.78	0.99	15.3	1.8	25	0.72
	1870A	0.00	-	-	-	0.00	-	-	-	-	0.00	-	-	-	-	0.24	13.3	1.1	11	0.00
	1870B	0.00	-	-	-	0.00	-	-	-	-	0.00	-	-	-	-	0.00	-	-	-	-
	1868	0.00	-	-	-	0.00	-	-	-	-	0.00	-	-	-	-	0.00	-	-	-	-
	2251	0.00	-	-	-	0.00	-	-	-	-	0.00	-	-	-	-	0.14	15.5	∞	0	0.00
2S1	3352	0.00	-	-	-	0.59	20.2	1.1	22	1.33	0.00	-	-	-	-	0.49	18.8	1.3	21	0.00
2S2	2123	0.00	-	-	-	0.12	23.5	0.9	32	0.47	0.00	-	-	-	-	0.05	-	-	-	-
	2259A	0.05	-	-	-	0.34	22.6	0.9	24	0.47	0.02	-	-	-	-	0.15	21.7	1.4	23	0.00
	2259B	0.01	-	-	-	0.37	23.4	0.9	26	0.60	0.01	-	-	-	-	0.17	22.3	1.4	23	0.00
	2627	0.00	-	-	-	0.25	22.8	0.9	23	0.69	0.00	-	-	-	-	0.13	21.7	1.3	22	0.00
2S3	2124	0.00	-	-	-	0.00	-	-	-	-	0.00	-	-	-	-	0.20	21.7	∞	0	0.00
	2628A	0.00	-	-	-	0.00	-	-	-	-	0.00	-	-	-	-	0.20	22.7	∞	0	0.00
	2628B	0.00	-	-	-	0.00	-	-	-	-	0.00	-	-	-	-	0.00	-	-	-	-
2S4	2125	0.00	-	-	-	0.00	-	-	-	-	0.00	-	-	-	-	0.00	-	-	-	-
	2261	0.00	-	-	-	0.00	-	-	-	-	0.00	-	-	-	-	0.00	-	-	-	-
	2633A	0.00	-	-	-	0.00	-	-	-	-	0.00	-	-	-	-	0.00	-	-	-	-
	2633B	0.00	-	-	-	0.00	-	-	-	-	0.00	-	-	-	-	0.00	-	-	-	-
3S1	2258	0.01	-	-	-	0.73	19.4	1.2	13	1.79	0.01	-	-	-	-	0.57	21.9	7.1	15	0.86
	2623	0.06	17.4	0.6	11	0.26	18.2	0.8	15	0.68	0.23	19.7	5.7	13	0.87	0.56	21.6	17.3	17	0.84
	3070	0.00	-	-	-	0.78	19.3	0.9	28	0.89	0.00	-	-	-	-	0.52	18.4	1.3	28	0.26
3S2	2257	0.00	-	-	-	0.00	-	-	-	-	0.00	-	-	-	-	0.02	-	-	-	-
	3071	0.00	-	-	-	0.30	26.8	2.5	31	2.45	0.00	-	-	-	-	0.14	21.9	1.5	28	0.52
3S3	2256	0.08	16.0	0.6	11	0.33	16.8	0.8	16	0.62	0.25	18.3	4.8	14	0.86	0.53	21.0	7.4	19	0.84
3S4	2255	0.00	-	-	-	0.00	-	-	-	-	0.00	-	-	-	-	0.10	19.0	∞	0	0.00
4S1	2670	0.20	18.9	0.6	5	0.70	19.9	1.0	9	1.28	0.21	20.0	4.8	6	0.93	0.61	21.8	10.5	10	0.90
4S2	2264	0.01	-	-	-	0.62	17.4	0.8	53	0.33	0.05	-	-	-	-	0.34	17.7	1.4	53	0.33
	2625	0.17	16.4	0.7	47	0.86	17.2	0.8	53	0.21	0.43	18.1	1.5	50	0.44	0.88	17.7	1.4	53	0.31
4S3	2262A	0.53	16.9	0.7	35	0.64	17.3	0.8	38	0.13	0.82	18.3	1.5	38	0.51	0.58	18.2	1.5	38	0.48
	2262B	0.45	17.3	0.7	44	0.42	17.7	0.8	46	0.10	0.53	18.5	1.4	46	0.40	0.27	18.5	1.4	46	0.38
	2636A	0.30	17.9	0.7	35	0.84	18.7	0.8	40	0.22	0.53	19.5	1.5	38	0.52	0.71	19.1	1.4	40	0.40
	2636B	0.08	18.0	0.7	40	0.89	19.0	0.8	46	0.27	0.20	19.8	1.6	43	0.50	0.68	19.3	1.4	46	0.32
4S4	2263A	0.00	-	-	-	0.17	27.1	4.0	35	3.15	0.00	-	-	-	-	0.57	21.9	4.8	31	0.73
	2263B	0.73	17.9	0.6	15	0.47	17.8	0.7	14	0.00	0.47	17.8	1.1	14	0.00	0.59	17.7	1.2	12	0.00
5S1	2254	0.00	-	-	-	0.00	-	-	-	-	0.00	-	-	-	-	0.00	-	-	-	-
	2626	0.00	-	-	-	0.00	-	-	-	-	0.00	-	-	-	-	0.00	-	-	-	-
	2849	0.39	17.2	0.6	0	0.22	17.2	∞	0	0.00	0.22	17.2	∞	0	0.00	0.30	17.9	21.1	2	0.98
	3068	0.12	16.3	0.6	25	0.85	17.2	0.8	30	0.35	0.25	17.9	1.6	28	0.66	0.65	17.5	1.4	30	0.52
I1	1889	0.03	-	-	-	0.31	17.8	0.9	103	0.17	0.49	19.7	1.7	101	0.27	0.54	19.3	1.6	103	0.23
I2	1890	0.20	18.8	0.7	60	0.09	18.7	0.8	59	0.00	0.12	19.7	1.4	62	0.23	0.14	20.4	1.6	60	0.39
I3	1771	0.00	-	-	-	0.00	-	-	-	-	0.00	-	-	-	-	0.25	12.3	1.1	6	0.00
I4	1888	0.24	17.1	0.8	169	0.32	17.8	1.0	175	0.07	0.85	19.4	1.6	175	0.10	0.57	19.5	1.7	175	0.10
I5	1886	0.87	16.6	0.7	111	0.93	16.9	0.9	114	0.04	0.77	17.0	1.3	112	0.05	0.73	16.8	1.4	113	0.00